Manuscript Details

Manuscript number	CHEMER_2018_67
Title	Carbon and nitrogen pools in Padanian soils (Italy): origin and dynamics of Soil Organic Matter
Article type	Research Paper

Abstract

Carbon and nitrogen elemental (C-N, wt%) and isotopic (δ13C-δ15N, ‰) investigation has been carried out on alluvial and deltaic soils from the Padanian plain (northern Italy), an area interested by intensive agricultural activities, in order to refine previous inferences on the depositional facies, on pedogenetic processes, as well as on anthropogenic influences. Soil analysis, carried out by EA-IRMS, have been focused on inorganic and organic fractions properly speciated by a thermally-based method, whereas further insights on the organic matter constituents have been obtained by sequential fractionation. The bulk EA-IRMS analyses reveals a remarkable compositional heterogeneity of the investigated soils (TC 0.89 to 11.93 wt%, TN 0.01 to 0.78 wt%, δ13C -1.2 to -28.2‰ , δ15N -1.2 to 10.0‰) that has to be explained as an integration between the inorganic and organic pools. The latter have been subdivided in Non-Extractable Organic Matter (NEOM, δ13C -16.3 to -28.6‰) and in extractable fractions as Fulvic (FA, δ13C -24.7 to -27.5‰, δ15N 0.6 to 5.7‰) and Humic (HA, δ13C -24.6 to -27.0‰, δ15N 1.0 to 9.7‰) Acids, which have been used to infer soil dynamics and Soil Organic Matter (SOM) stability processes. Results indicate that SOM at depth of 100 cm was generally affected by microbial reworking, with the exception of clayey and peaty deposits in which biological activity seems inhibited. Peaty and clayey soils displays an organic fraction loss of ca. 20% toward the surface, suggesting deterioration possibly induced by intensive agricultural activities. These latter may be the cause of the ubiquitous losses of organic fraction throughout the investigated area over the last eighty years, evaluated by the comparison with historical data on corresponding topsoils. The obtained insights are very important because these soils are carbon (and nitrogen) sinks that are vulnerable and can be degraded, loosing agricultural productivity and potentially contributing to greenhouse gases fluxes.

Keywords	agricultural soils; C-N isotopes; organic and inorganic pools; SOM dynamics

Corresponding Author	Gianluca Bianchini
Corresponding Author's Institution	University of Ferrara
Order of Authors	Claudio Natali, Gianluca Bianchini, Livia Vittori Antisari, Marco Natale, Umberto Tessari

Suggested reviewers	Alberto Agnelli, kazem zamanian

Submission Files Included in this PDF

File Name [File Type]

Cover Letter.docx [Cover Letter]

Natali et al. ChemderErde 2018.docx [Manuscript File]

Fig 1_new.pdf [Figure]

Fig 2.pdf [Figure]

Fig 3 abc_new.pdf [Figure]

Fig_4 Soils_new.pdf [Figure]

Fig 5_OM_Spec.pdf [Figure]

Fig 6 HA-FA.pdf [Figure]

Fig 7.pdf [Figure]

Table 1_rev.pdf [Table]

Table 2_rev_new.pdf [Table]

Table 3_rev_new.pdf [Table]

Supplementary Fig 1_new.pdf [e-Component]

Supplemenetary Table 1_rev.pdf [e-Component]

Supplemenetary Table 2.pdf [e-Component]

To view all the submission files, including those not included in the PDF, click on the manuscript title on your EVISE Homepage, then click 'Download zip file'.

Research Data Related to this Submission

There are no linked research data sets for this submission. The following reason is given:
Data will be made available on request

Dear Editor,

we are sending you a manuscript titled "**Carbon and nitrogen pools in Padanian soils (Italy): origin and dynamics of Soil Organic Matter**". It includes 84 C and N elemental and isotopic analyses (obtained with a new EA-IRMS system set in our Labs) on soils that were previously studied for major and trace element composition (e.g., Di Giuseppe et al., 2014; Chemie der Erde – Geochemistry).

We think that these new data are important because they provide a better understanding of the Soil Organic Matter , which dynamic is of fundamental importance to evaluate soil fertility and their potential impact on GHG emissions.

We hope that you will judge the content suitable for the Journal and we remain at your disposal for any editorial requirement.

Sincerely,

Gianluca Bianchini, Claudio Natali and Co-Authors

Carbon and nitrogen pools in Padanian soils (Italy): origin and dynamics of Soil Organic Matter

Natali C.[a], Bianchini G.[a,*], Vittori Antisari L.[b], Natale M.[b], Tessari U.[a]

[a]Department of Physics and Earth Sciences, University of Ferrara, Italy

[b]Department of Agricultural and Food Sciences, Alma Mater Studiorum, University of Bologna, Italy

***Corresponding author: Gianluca Bianchini**

Dept. of Physics and Earth Sciences, University of Ferrara, via Saragat 1, 44122, Ferrara - Italy

Phone: +39 328 7429382

E-mail: bncglc@unife.it

Abstract

Carbon and nitrogen elemental (C-N, wt%) and isotopic ($\delta^{13}C$-$\delta^{15}N$, ‰) investigation has been carried out on alluvial and deltaic soils from the Padanian plain (northern Italy), an area interested by intensive agricultural activities, in order to refine previous inferences on the depositional facies, on pedogenetic processes, as well as on anthropogenic influences. Soil analysis, carried out by EA-IRMS, have been focused on inorganic and organic fractions properly speciated by a thermally-based method, whereas further insights on the organic matter constituents have been obtained by sequential fractionation. The bulk EA-IRMS analyses reveals a remarkable compositional heterogeneity of the investigated soils (TC 0.89 to 11.93 wt%, TN 0.01 to 0.78 wt%, $\delta^{13}C_{TC}$ -1.2 to -28.2‰ , $\delta^{15}N$ -1.2 to 10.0‰) that has to be explained as an integration between the inorganic and organic pools. The latter have been subdivided in Non-Extractable Organic Matter (NEOM, $\delta^{13}C$ -16.3 to -28.6‰) and in extractable fractions as Fulvic (FA, $\delta^{13}C$ -24.7 to -27.5‰, $\delta^{15}N$ 0.6 to 5.7‰) and Humic (HA, $\delta^{13}C$ -24.6 to -27.0‰, $\delta^{15}N$ 1.0 to 9.7‰) Acids, which have been used to infer soil dynamics and Soil Organic Matter (SOM) stability processes. Results indicate that SOM at depth of 100 cm was generally affected by microbial reworking, with the exception of clayey and peaty deposits in which biological activity seems inhibited. Peaty and clayey soils displays an organic fraction loss of ca. 20% toward the surface, suggesting deterioration possibly induced by intensive agricultural activities. These latter may be the cause of the ubiquitous losses of organic fraction throughout the investigated area over the last eighty years, evaluated by the comparison with historical data on corresponding topsoils. The obtained insights are very important because these soils are carbon (and nitrogen) sinks that are vulnerable and can be degraded, loosing agricultural productivity and potentially contributing to greenhouse gases fluxes.

Keywords: agricultural soils; C-N isotopes; organic and inorganic pools; SOM dynamics

1 Introduction

The Padanian Plain (northern Italy), is the sedimentary basin bordered by the Alps and the Apennines, which hosts about 30–40% of the Italian population and most of the Nation's industrial and agricultural activities. The geochemistry of its sediments, of Holocene age, records an interplay between tectonic, climatic and hydrological processes. These sediments have been investigated by several papers which were mainly focused on the inorganic constituents that represent useful proxies to understand the provenance of the clastic particles and the relationships with the depositional environment (Amorosi et al., 2002; Bianchini et al., 2002; Amorosi, 2012; Bianchini et al., 2012; 2013; 2014; Di Giuseppe et al., 2014a; 2014b). However, these papers never described the associated organic fraction which is fundamental to understand the occurring pedogenetic processes. In this framework, this work aims to complement the previous investigations providing for the first time systematic carbon and nitrogen elemental and isotopic analyses of soils from the easternmost Padanian plain. In particular, inorganic (TIC) and organic (TOC) soil carbon pools have been characterized by EA-IRMS on the basis of their thermal behavior (Natali et al., 2018). The Soil Organic Matter (SOM) has been investigated separating the non-extractable and extractable components (humin, humic and fulvic acids; Ciavatta et al., 1990) which have been analyzed for their C and N elemental and isotopic composition. The presented data are essential to define the C-N pools coexisting -at different extent- in the distinct sedimentary facies, to understand the soil development and the biogeochemical cycles occurring in the investigated environmental-agricultural system. The data provide insights on organic matter dynamics and transformation and allow to estimate the soil nutrient storage capacity in relation to the existing agricultural activities. The approach is also useful to evaluate the SOM evolution and the related effects on carbon sequestration and/or greenhouse gases release of the investigated soils (e.g. Albaladejo et al., 2013; Ogrinc et al., 2015).

2 Geological and geomorphological framework

The soils of the easternmost Padanian Plain developed from alluvial (and deltaic) deposits; they are characterized by a limited profile development, in which the lack of soil maturity is related to young depositional age (Holocene), fluvial reworking and extensive agricultural activities (ploughing). In the studied area, located in the neighbors of the town of Argenta (province of Ferrara), the outcropping sedimentary facies (and the related soils) reflect climatic changes and human impacts that deeply modified the configuration of the local drainage system, which is mainly represented by the migrating branches of the Po river (Bondesan et al., 1995; Stefani and Vincenzi, 2005; Simeoni and Corbau, 2009). In the same sector of the plain, sediments of Apennine provenance transported in historical times by River Reno are also represented, giving further complexity to the geomorphological evolution of the plain, in turn reflected in the sediment stratigraphy. In the terminal part of the basin the delta environment is characterized by high lateral mobility of the active channel belts, with recurrent avulsion and channel bifurcation, which redistributes the water and sediment fluxes throughout the system. This dynamic scenario permitted, in historical times, the development of fens and swamps (probably developed over the period of a few decades) sometimes characterized by peat deposition (Di Giuseppe et al., 2014a; 2014b). Some of these wetlands possibly received sedimentary contributions from both the Po and Reno riverine systems, as already observed in other sectors of the easternmost Padanian plain (Bianchini et al., 2014).

The studied soils belong to the Inceptisols order and their classification highlights their origin from reclamation land. The largest group is Aquic Haplusteps (17 soil samples), followed by Udifluventic Haplustept (8 soil samples), Sulfic Endoaquepts (6 soil samples), then Vertic Endoaquepts (3 soil samples). Entisols are also recognized as Oxyaquic Ustifluvents (SSS, 2010). Pedological features and soil taxonomy is reported in Supplementary Table 1.

3 Investigated materials and analytical methods

3.1 Soil samples

The samples considered in this study were selected from a samples collection previously studied by Di Giuseppe et al. (2014c), which presented a complete set of major and trace element analyses carried out by X-Ray Fluorescence (XRF). The samples have been collected around the town of Argenta (44°36'47"N, 11°50'11" E; Fig. 1) in which the different alluvial (and deltaic) facies of the Po and Reno rivers were identified. At each sampling site two samples were collected: one close to the surface (labelled *A*) representative of the plough horizon (just beneath the roots zone; depth 20–30 cm) and the other representative of the underlying undisturbed layer (depth 100–120 cm, labelled *B*). In this new study, 47 soil samples have been reconsidered for carbon and nitrogen analyses. In particular, 38 *B* samples were selected to investigate the C and N background, at a depth not affected by mechanical disturbance. For 11 selected sites, the study of the above mentioned subsoils has been coupled with that of the respective superficial layer in order to account for the effect of agricultural practices (ploughing, fertilizers and crops). Moreover, textural analyses have been carried out on a subset of samples and the related results are reported in Supplementary Table 2.

3.2 EA-IRMS analysis

The elemental and isotopic carbon composition of the different carbon and nitrogen pools have been carried out by the use of an Elementar Vario Micro Cube Elemental Analyzer in line with an ISOPRIME 100 Isotopic Ratio Mass Spectrometer operating in continuous-flow mode. The system allows variations of the combustion module temperature up to 1050°C; this permits extraction of different components having distinctive destabilization temperatures and to analyze the respective C, N (wt%) and $^{13}C/^{12}C$, $^{15}N/^{14}N$ ratios (R) notionally expressed as $\delta(‰) = (1000*[R_{sample}-R_{standard}]/$

$R_{standard}$), relative to the international isotope standard that are Pee Dee Belemnite (PDB) for carbon and AIR for nitrogen (Gonfiantini et al., 1995).

Powdered samples are introduced in tin capsules that are wrapped and weighed; these capsules, that allow to load up to 40 mg of sample, are subsequently introduced in the Vario Micro Cube autosampler to be analyzed. Flash combustion takes place in a sealed quartz tube filled with copper oxide grains (padded with corundum balls and quartz wool) which acts as catalyst, in excess of high purity (grade 6.0) O_2 gas. Freed gaseous species are transferred through a reduction quartz tube (at 550°C) filled with metallic copper wires that reduce the nitrogen oxides (NO_x) to N_2. The formed analyte gases (N_2, H_2O and CO_2), carried by dry He (grade 5.0) gas, pass through a water-trap filled with Sicapent ensuring complete removal of moisture, are sequentially separated by a temperature programmable desorption column (TPD) and quantitatively determined on a thermal-conductivity detector (TCD). Sample N_2 goes directly to the interfaced IRMS for isotopic composition determination, while CO_2 is held by the TPD column, kept at room temperatures 20–25°C. When N_2 isotopic analysis is over, CO_2 is desorbed from the TPD column raising the temperature to 210°C, and finally reaches the IRMS compartment for the determination of carbon isotopic ratios. The detection of the distinct isotopic masses of the sample are sandwiched between those of reference N_2 and CO_2 (5 grade purity) gases, which have been calibrated using a series of reference materials, in turn calibrated against IAEA international standards, such as the limestone JLs-1 (Kusaka and Nakano, 2014), the peach leaves NIST SRM1547 (Dutta et al., 2006), the Carrara Marble (calibrated at the Institute of Geoscience and Georesources of the National Council of Researches of Pisa), and the synthetic sulfanilamide provided by Isoprime Ltd. Mass peaks were recalculated as isotopic ratios by the Ion Vantage software package. Reference and carrier gases of certified purity were provided by SIAD Ltd.

Precision of elemental concentration measurement were estimated by repeated analyses of the standards, and accuracy estimated by the comparison between reference and measured values, were

in the order of 5% of the absolute measured value. Uncertainties, increase for contents approaching the detection limit (0.001 wt %). Carbon and nitrogen isotope ratios are expressed in the standard (δ) notation in per mil (‰) relative to the international Vienna Pee Dee Belemnite (V-PDB) and atmospheric air (AIR) isotope standards (Gonfiantini et al., 1995). The $\delta^{13}C$ and $\delta^{15}N$ values were characterized by an average standard deviation (1 sigma) of ±0.1‰ and ±0.3‰, respectively as defined by repeated analyses of the above mentioned standards.

3.3 Discrimination of soil inorganic and organic pools

The elemental and isotopic compositions of the of Total Carbon (TC), Organic Carbon (TOC), Inorganic Carbon (TIC) and the associated nitrogen fractions, have been carried out according to the method proposed by Natali and Bianchini (2014; 2015), that was specifically refined for soil samples by Natali et al. (2018). According to this analytical protocol:

- TC (and TN) was carried out by EA-IRMS combusting at 950°C the bulk sample;

- TOC was carried out by EA-IRMS combusting at 500°C the bulk sample;

- TIC was carried out by EA-IRMS combusting at 950°C the sample deprived of organic matter, i.e. preliminary burnt in a muffle furnace at 550°C for 12h; the relative gravimetric loss (LOI) is also determined in order to correct the elemental concentration of the TIC fraction.

The resulting wt% and $\delta^{13}C$ (‰) of the OC and IC fractions allow a mass balance to calculate a theoretical TC fingerprint which is compared with that directly measured ($\delta^{13}C_{TC\ Measured}$):

$$\delta^{13}C_{TC\ Theoretical} = (\delta^{13}C_{TOC} * X_{TOC} + \delta^{13}C_{TIC} * X_{TIC})/(X_{TOC} + X_{TIC})$$

where X_{TOC} and X_{TIC} represent the organic and inorganic fractions, respectively.

The difference between theoretical and measured bulk isotopic ratios, expressed as $\Delta^{13}C$, complements the elemental carbon recovery and is used to cross-check the reliability of the method:

$$\Delta^{13}C = \delta^{13}C_{TC\ Measured} - \delta^{13}C_{TC\ Theoretical}$$

On a subset of 15 samples, the SOM has been chemically separated in Non-Extractable Organic Matter (NEOM), Humic and Fulvic Acids (HA and FA, respectively) using a strongly chelating high pH solution according to Vittori Antisari et al. (2010). Briefly, 10g of soil were placed in a 250ml teflon bottle adding 100ml of 0.1M $Na_4P_2O_7$ plus 0.1M NaOH solution and shaken in a Dubnoff water bath for 24h at 65°C. Afterwards, the samples were centrifuged at 7000 rpm for 20 minutes and the supernatant was separated from the mineral fraction. The extracted solution was filtered at 0.45 μm with Millipore vacuum filter. The total extracted solution were acidified at pH value lower than 2 using 6M HCl, in order to force the HA precipitation. After centrifugation at 8000 rpm for 20 minutes the HA were isolated, then were re-dissolved with 0.5M NaOH solution. This last step has been repeated three times. The FA fraction was separated by no-humic compounds using solid chromatography techniques with polyvinilpirrolidone (PVP) following the procedures given in Ciavatta et al., 1990. The HA and FA fractions were purified using Spectra-por dialyzing membranes (MWCO 6000-8000 Da and 1000 Da, for HA and FA, respectively), after dialysis the purified samples were freeze-dried and lyophilized.

4 Results

4.1 C and N elemental and isotopic soil composition

The total carbon (TC) and nitrogen (TN) elemental and isotopic analyses have been carried out on 39 subsoil (*B*) samples at 100-120 cm depth in order to define the natural background and to characterize different depositional facies. The analyses, reported in Table 1, highlight that subsoils are characterized by a wide elemental and isotopic compositional variability. In particular, TC ranges from 0.89 wt% (AR8B) to 11.93 wt% (AR38B) and TN from 0.01 wt% (AR25B) to 0.78 wt% (AR38B). The isotopic composition of the investigated subsoils showed $\delta^{13}C_{TC}$ values varying

from -28.2‰ (AR38B) to -1.2‰ (AR25B) whereas the $\delta^{15}N$ values range between -0.7‰ (AR15B) and 6.8‰ (AR13B). Bivariate statistical analysis based on Pearson correlation shows that TN is negatively correlated with $\delta^{13}C_{TC}$ value (r=-0.84) whereas no other significant correlation among these variables have been observed.

These C and N data have been also compared with the major and trace elements (obtained by XRF) reported for the same samples by Di Giuseppe et al. (2014c) and the resulting correlation matrix highlight that TC is positively correlated with CaO (r=0.73) and to a lesser extent with Sr (r=0.66), suggesting a significant presence of carbonates in these soils. This is confirmed by the significant ($p<0.05$) negative correlation of TC with other elements typically contained in silicates (e.g. Pb r=-0.73, Rb r=-0.71 and Th r=-0.70) as well as by the parallel positive correlation of $\delta^{13}C$ with CaO (r=0.75) and Sr (r=0.73). Moreover, the carbon isotopic ratio displays a well-defined negative correlation with Al_2O_3 (r=-0.73), K_2O (r=-0.74), Pb (r=-0.71), Cu (r=-0.74), and to a lesser extent with Rb (r=-0.69), V (r=-0.67), Zn (r=-0.68) and Th (r=-0.62) which are all elements typically contained in phyllosilicates and/or bound to organic matter that is generally predominant in the soil fine fractions.

A hierarchical cluster analysis has been carried out combining the new data (TC, TN, $\delta^{13}C_{TC}$) with the pre-existing XRF analyses (Di Giuseppe et al., 2014c). The results suggest that the sample population can be subdivided in 4 groups that broadly conform to the distinct depositional facies highlighted by Di Giuseppe et al., 2014a (P – paleochannels, L – levees, M – marshes, S – swamps).

The soils grouped by P cluster are characterized by shallow water table, formed in alluvium and receive high moisture (e.g. Udifluventic Haplustepts and Oxyaquic Ustifluvents); they are characterized by the following averaged values: C = 2.88 wt%, N= 0.02 wt%, $\delta^{13}C_{TC}$ = -1.8 ‰, $\delta^{15}N$ = 3.0 ‰.

The soils grouped by L cluster are formed under redox depletion with low chroma commonly in a brownish or reddish matrix in the subsoil (Aquic Haplustepts); they are characterized by the following averaged values: C = 2.50 wt%, N= 0.05 wt%, $\delta^{13}C_{TC}$ = -4.8 ‰, $\delta^{15}N$ = 2.4 ‰.

The samples grouped in the cluster M are soils typically derived from coastal marshes in riverine deltas (e.g. Terric Sulfisaprists and Sulfic Endoaquepts); they are characterized by the following averaged values: C = 2.91 wt%, N= 0.13 wt%, $\delta^{13}C_{TC}$ = -10.9 ‰, $\delta^{15}N$ = 3.1 ‰.

The samples grouped in the cluster S are soils characterized by silty clay textured alluvium deposit, formed in internal deltaic sectors of the Po riverine system (Aquic Calciusteps, Sulfic Endoaquepts); they are characterized by the following averaged values: C = 3.34 wt%, N= 0.11 wt%, $\delta^{13}C_{TC}$ = -21.3 ‰ $\delta^{15}N$ = 4.2 ‰. We included in this group the unclusterized sample AR38 (Fluvaquentic Endoaquolls), showing an extreme C and N content (TC = 11.93 wt%, N = 0.78 wt%) coupled with very ^{13}C depleted isotopic composition ($\delta^{13}C_{TC}$ = -28.2 ‰).

Coherently, the compositional variation of the identified sample groups in terms of TC, N, and $\delta^{13}C_{TC}$ is reported in Fig. 2. These clusters obtained elaborating chemical and isotopic data, roughly discriminate distinct textural groups, as evidenced by the Sand-Silt-Clay ternary diagram of Supplementary Fig. 1.

The new data potentially provide constraints on the carbon and nitrogen pools of the investigated soils. In particular, the distribution of TC, $\delta^{13}C_{TC}$ vs CaO and Sr/Rb are useful to identify the main mineral and organic components that induce the observed variation (Figure 3). In Fig. 3a (CaO vs TC), some samples straddle along calcite stoichiometric line (clusters L) suggesting that carbonate represents the main C pool. Other samples plot on the right of the calcite stoichiometric line (clusters M and S) because they contain a significant amount of OM and/or authigenic minerals such as oxalate. Only few samples plot on the left of the calcite stoichiometric line suggesting a variable contribution by CaO-bearing silicate minerals such as feldspars (cluster P). In Fig. 3b (CaO

vs $\delta^{13}C_{TC}$), most samples are distributed along the mixing line between primary carbonates (typically characterized by CaO 12 wt% and $\delta^{13}C_{TC}$ approaching 0‰) and CaO-free OM that conforms to C3 photosynthetic pathway vegetation ($\delta^{13}C$ ca. -27‰, De Niro and Epstein, 1990). However, some samples (cluster M) deviate from this hyperbolic mixing trend suggesting the presence of a further CaO-bearing end-member characterized by ^{13}C depleted isotopic composition, possibly consisting of oxalate or authigenic carbonate and/or sulphates (Dauer and Perakis, 2014; Kovda et al., 2014). Fig. 3c, reporting Sr/Rb vs $\delta^{13}C_{TC}$, confirms that most of the samples can be interpreted as mixing of OM-free coarse sediments and OM-rich fine sediments. However, even in this case some samples (cluster M) are displaced from this trend suggesting the presence of a third end-member possibly consisting of oxalates and authigenic carbonates and/or sulphates.

A subset of 11 superficial (*A*) soils representative of the plough horizon (20-30 cm depth) have been also analyzed and the results have been compared with their respective *B* subsoils with the aim of delineate the carbon and nitrogen variability along with the depth profile, and to emphasize the possible existence of Top Enrichment Factors (TEF), calculated as the ratio between topsoil and subsoil concentrations (Ungaro et al., 2008), related to anthropogenic activities. The elemental analyses reveal that the average TC content of the sampled soils is slightly higher in the *A* horizon (3.35 wt%) than in the and the *B* layer (2.73 wt%), although extreme compositions exist at both depths (SD of 1.29 and 2.94, respectively). Accordingly, the average TEF is 1.3 possibly reflecting the presence of OM derived from both crop residua or organic fertilizers (e.g., manure or slurry) reincorporated in the soil by tillage. The whole carbon isotopic composition is decidedly more negative in the *A* (average $\delta^{13}C_{TC}$ -14.3 ‰) with respect to the relative *B* (average $\delta^{13}C_{TC}$ -8.3 ‰) samples, with the exception of two *B* samples characterized by ^{13}C-depleted composition (AR38B $\delta^{13}C_{TC}$ -28.2 ‰; AR41B $\delta^{13}C_{TC}$ -25.2 ‰) in relation to their peculiar pedological characters (Fluvaquentic Endoaquolls and Sulfic Endoaquepts, respectively).

Coherently, the total nitrogen elemental content (TN) is higher in the *A* (average 0.20 wt%) with respect to *B* (average 0.09 wt%) samples, which implies an average TEF of 2.4. The associated nitrogen isotopic composition shows average $\delta^{15}N$ of 5.7 ‰ in *A* and of 2.9 ‰ in *B* samples. Noteworthy, the TN negatively correlates with $\delta^{13}C_{TC}$ and the highest TN content is detected in the above mentioned *B* sample AR38B (0.78 wt%).

4.2 Organic vs Inorganic carbon pools

The elemental and isotopic TOC and TIC determinations have been carried out on 20 samples (13 *B* subsoils and 11 *A* topsoils), representative of the different depositional facies delineated above. The results are reported in Table 2, which also includes the calculated elemental and isotopic carbon recoveries, and in Fig. 4. TOC average is 1.8 wt% in *A* samples and 0.6 wt% in *B* samples, which corresponds to a TOC fraction of ca. 52% of the TC in the *A* samples that is decidedly higher than that recorded in *B* samples (TOC ca. 35% of the TC). The average TOC isotopic composition ($\delta^{13}C_{TOC}$) of the *A* topsoils is -24.8 ‰, showing a $\delta^{13}C$ depletion of ca. 2.5 ‰ with respect to that associated with *B* subsoils (average $\delta^{13}C_{TOC}$ = -22.3 ‰). A notable exception is represented by the two samples AR41B and AR38B in which TOC is nearly 90% of the TC, and characterized by comparatively more negative $\delta^{13}C_{TOC}$ values (-26.0 and -27.9 ‰, respectively).

The average TIC is similar in the *A* (1.7 wt%, SD = 0.8) and *B* (1.9 wt%, SD = 0.8) samples, but it represents different proportion with respect to the TC. Average TIC fraction is lower in the *A* (ca. 48% of the TC) with respect to that of the *B* samples where it account for ca. 65% of the TC; in organic-rich samples AR41B and AR38B it accounts for 5.0% and 0.2%, respectively. The average TIC isotopic composition ($\delta^{13}C_{TIC}$) is slightly more depleted in ^{13}C in the *A* topsoils ($\delta^{13}C_{TIC}$ = -3.1 ‰, SD =1.8) with respect to that recorded in the *B* undisturbed layer ($\delta^{13}C_{TIC}$ = -4.2 ‰, SD =5.5). Some decidedly negative isotopic values are observed in the topsoil AR16A ($\delta^{13}C_{TIC}$ = -6.7 ‰) and in the subsoils of the S group ($\delta^{13}C_{TIC}$ from -8.8 to -19.4 ‰), plausibly resulting from the presence of authigenic minerals (oxalate and/or carbonates, Milliere et al., 2011; Lawrence et al., 2015;

Zamanian et al., 2016), or from the existence of thermally recalcitrant OM compounds (Johnson et al., 2016).

As concerns the variation of the soil carbon pools in different depositional facies (defined only for subsoils), the TOC fraction respect to the TC increases from P (average of 6%), to L and M (average of 16% and 42%, respectively), reaching extreme values in S samples (average of 87%). The associated isotopic composition ($\delta^{13}C_{TOC}$) ranges around -22 ‰ in L and M samples, and becomes decidedly more negative in S samples (average of -26.1 ‰). Analogies are observed in the isotopic composition of the TIC fraction that is comparable in L and M samples ($\delta^{13}C_{TIC}$ around -1.8 ‰) and becomes decidedly more negative in the S samples (average $\delta^{13}C_{TIC}$ -13 ‰).

4.3 Carbon (and Nitrogen) speciation of Organic Matter

The SOM characterization has been carried out on a subset of 15 samples (8 from the *B* and 7 from the *A* horizons) by carbon isotopic analyses of the chemically non-extractable organic matter (NEOM) and of extracted fulvic (FA) and humic acids (HA, Table 3 and Fig. 5). The carbon isotopic composition of NEOM in *B* samples is generally more ^{13}C-enriched (average of -18.9 ‰) than that of *A* samples (average of -20.8 ‰), with the exception of the organic-rich samples AR38B ($\delta^{13}C_{NEOM}$ = -28.6 ‰) and AR41B ($\delta^{13}C_{NEOM}$ = -24.3 ‰).

The carbon isotopic composition of extractable OM pools (EOM) is rather homogeneous in soils both from the *B* and *A* horizons. In particular, FA shows an average $\delta^{13}C_{FA}$ of -25.3‰ (SD=0.7‰) and $\delta^{13}C_{FA}$ of -26.2‰ (SD=0.8‰) for the *B* and *A* samples, respectively. These values are slightly ^{13}C-enriched in comparison with those obtained for HA which show average $\delta^{13}C_{HA}$ of -25.7‰ (SD=0.8‰) in the *B* soils and of -25.8‰ (SD=0.9‰) in *A* soils. On the whole, the nitrogen isotopic composition shows distinctly higher values in HA (average of $\delta^{15}N_{HA}$ = 4.8 ‰) respect to that recorded in FA (average of $\delta^{15}N_{FA}$ = 2.3 ‰). The nitrogen isotopic composition of both the extractable OM pools also exhibit a marked ^{15}N depletion with depth (Fig. 6). In particular,

averaged $\delta^{15}N$ values in HA decrease from 6.3 ‰ (SD = 1.5 ‰) in *A* samples to 3.4 ‰ (SD = 0.8 ‰) in *B* samples, whereas FA show a less marked variation ($\delta^{15}N_{FA}$ = 2.9 ‰, SD=1.8 ‰ for *A* soils and $\delta^{15}N$ = 1.8 ‰, SD=1.4 ‰ for *B* soils).

Noteworthy, there are differences in the carbon isotopic composition of SOM pools in samples pertaining to distinct depositional facies. The $\delta^{13}C_{NEOM}$ generally shows the less negative values in L samples (up to -16.3 ‰ in AR19B), a tendency toward more negative values in M samples (average of -20.0 ‰), and the more ^{13}C-depleted values in S samples (down to -28.6 ‰ in AR38B). The differences in terms of carbon isotopic composition of SOM extractable pools ($\delta^{13}C_{EOM}$) among the distinct soil groups are less marked, although the S sample AR38B is invariably characterized by the more $\delta^{13}C$ values (down to -27.0 ‰ in HA, -27.4 ‰ in FA).

5 Discussion

5.1 Insights from the Inorganic carbon fraction

The elemental and isotopic carbon speciation of the studied soils allows to investigate the nature of the carbonatic fraction included the Padanian alluvial plain sediments. From one hand, where organic matter is subordinate, the isotopic fingerprint of the TIC maintains reliable information on the composition of primary carbonate mother rocks, allowing a possible distinction among different sources and provenance. From another hand, where organic matter become prevalent, the carbon isotopic fingerprint of the TIC allows to check the involvement of organic matter in biomineralization processes and/or formation of secondary pedogenic carbonates.

The inorganic carbon fraction and the associated isotopic composition of the investigated soils show a bimodal distribution: most of the samples show a narrow range of ^{13}C-enriched isotopic composition ($\delta^{13}C_{TIC}$ from -1.5 to -4.2‰) which is associated with a broad TIC fraction varying in

the range 45-85% of the TC, whereas TOC-rich samples (70-98% of the TC, generally ascribed to the S group) are characterized by a distinctly negative $\delta^{13}C_{TIC}$ range (from -8.8 to -19.4‰). The predominant group shows a TIC isotopic composition which is compatible with that of sedimentary marine carbonates supplied by the drainage network during the development and progradation of the alluvial plain, whereas the subordinate group -including samples AR8B, AR38B, AR41B and AR16A- show $\delta^{13}C_{TIC}$ values similar to that recorded in palustrine carbonates developed in a swampy environment (Alonso-Zarza et al., 2006; Dunagan and Turner, 2004). In these samples, the soil dynamics are particularly complex due to cyclic waterlogged and drained conditions which could produce variable interaction of carbonates with the organic matter as reflected by the difference obtained by the respective isotopic ratios ($\Delta^{13}C_{TIC\text{-}TOC}$) which range from -9.3 to -15.6 ‰ (Table 2). Therefore, the TIC isotopic composition of these samples, can be considered a proxy of a peculiar low-energy depositional environment typical of the reclaimed wetlands.

5.2 Insights from the organic pools

The SOM content is generally more abundant in *A* samples with respect to the deeper *B* samples. However, the more negative bulk $\delta^{13}C_{TC}$ of *A* topsoils respect to *B* subsoils, cannot be simply ascribed to an higher SOM content. In fact, in the investigated soils more negative SOM carbon isotopic ratios are characteristic of *A* samples (average $\delta^{13}C_{TOC}$ -24.7 ‰) with respect to *B* samples (average $\delta^{13}C_{TOC}$ -22.0 ‰), with the exception of the S samples showing the most negative ($\delta^{13}C_{TOC}$ from -24.4 to -28.7 ‰). According to De Clercq et al. (2015), this suggests a lower SOM maturity at the surface.

The NEOM carbon isotopic ratio is more ^{13}C-enriched in *B* samples ($\delta^{13}C_{NEOM}$ -18.9‰ on average) with respect to *A* samples ($\delta^{13}C_{NEOM}$ -20.8‰ on average) probably due to multiple biologically-driven reactions producing fugitive isotopic light compounds, and leaving a ^{13}C-enriched residual OM (Rumpel and Kögel-Knabner, 2010).

HA and FA are both strongly ^{13}C-depleted and don't display significant variation with depth. It is noteworthy that FA are generally characterized by slightly ^{13}C-depleted carbon isotopic ratios with respect to HA (average $\delta^{13}C$ -25.3‰ and -26.2‰, respectively) suggesting that they represent the extreme stage of SOM evolution, as also suggested by other studies (Agnelli et al., 2014).

In general, we observe a higher C isotopic difference ($\Delta^{13}C_{NEOM-EOM}$) between non-extractable and extractable organic matter in *B* (average of -6.7‰) with respect to *A* (average of -5.1‰) soils, with the exception of samples belonging to the S group that are characterized by the lowest $\Delta^{13}C_{NEOM-EOM}$ (AR38B +1.4‰, AR41B -1.6‰). This suggests that *B* soils underwent a higher biogeochemical processing, whereas *A* soils are fed by "fresh" OM still unaffected by microbial reworking (De Clercq et al., 2015). The paucity of fractionation observed in the OM compounds of the two S subsoils plausibly reflects their Aquic and Sulfic character which precludes high rate of microbial activity.

The carbon isotopic compositional differences observed among HA and FA, are remarked by nitrogen isotopic ratios, that are more ^{15}N enriched in HA with respect to FA (average $\delta^{15}N$ 4.8 ‰ and 2.3‰, respectively). This fractionation should be associated to biogeochemical processes leading to their intrinsic formation or by a higher attitude of FA to exchange/incorporate synthetic nitrogen derived by inorganic fertilization with respect to HA. The systematic ^{15}N-depletion of nitrogen isotopic ratios of HA and FA in deep (average $\delta^{15}N$ 3.4‰ and 1.8‰, respectively) with respect to superficial (average $\delta^{15}N$ 6.3‰ and 2.9‰, respectively) samples, reflects the downward migration of inorganic compounds employed as fertilizers ($\delta^{15}N$ ca. 0). This is coherent with other studies of the same agricultural area which emphasized the progressive leaching and percolation of N compounds along the soil profile (Colombani et al., 2011).

The current conditions of SOM in the investigated soils is summarized in Fig. 7 which reports the averaged compositions of bulk OM and of the related non-extractable and extractable fractions. In

general, the study emphasizes that although the SOM is quantitatively more abundant in the superficial horizon, its stability is lower than that from deeper horizon. In particular, labile and isotopically lighter organic compounds tend to concentrate at the surface, probably as a result of combined mechanical and agro-chemical effects.

On the whole, the isotopic composition of soil carbon OM pools seems to be correlated with the pedological characters, which in turn reflect the depositional facies and the post-sedimentary evolution, which also includes anthropogenic activities. The SOM dynamics is expressed as a function of the isotope composition of the different carbon pools such as NEOM, HA and FA. The isotopic decoupling between NEOM and HA-FA (expressed by $\Delta^{13}C_{NEOM\text{-}EOM}$ ‰) is very similar in *A* samples (average of -5.1 ‰, SD = 1.0 ‰), whereas it shows a marked variations in *B* samples (average of -6.7 ‰, SD = 3.8 ‰), reflecting the more complex evolutionary conditions of deep undisturbed soil horizons with respect to the plough horizon. In particular in *B* soils, $\Delta^{13}C_{NEOM\text{-}EOM}$ display a significant positive correlation (r^2 = 0.83) with the TOC (%), suggesting that soil samples having TOC higher than 90% undergone minimum SOM transformation and evolution ($\Delta^{13}C_{NEOM\text{-}EOM}$ around 0‰). This is the case of the TOC-rich samples of the S group, that although very different in terms of geochemical and grain size compositions, show similar hydromorphic pedological features (Aquic to Sulfic) that prevent SOM processing and evolution.

The SOC variation along the soil profile in the different depositional facies has been estimated by the difference of organic carbon percentages in *A* soils with respect to that in *B* subsoils. It can be systematically observed that the L group is enriched (20-77 %) and S group is depleted (from -13 to -25 %) in TOC at surface, whereas intermediate and more variable conditions characterize M samples. This imply that, in spite of the agricultural activities that add organic matter, S soils are affected by TOC losses at surface, which can be mainly attributed to oxidation induced by intensive agricultural practices.

Carbon losses can be estimated also by comparison with historical data that have been retrieved for a subset of sampling sites from an agronomic archive available at the Department of Agricultural and Food Sciences of the University of Bologna, including soil analyses carried out before war world two. This comparison highlights that the organic carbon fraction has been reduced at all sites, recording losses up to 30% over the last eighty years.

Particular attention has to be paid to the peaty deposits that show distinctive features, diverging from most of the other samples and indicating peculiar SOM evolutionary processes; their SOM decomposition, with relative CO_2 emission in atmosphere, is potentially enhanced by wetland reclamation and agricultural activities that led them to undergo highly oxidative conditions (Hooijer et al., 2010). The related soil profile shows depletion of organic matter content toward the surface and temporal loss of the organic carbon fraction, estimated as 10-15% during the last eighty years.

6 Conclusions

This paper implements previous geochemical studies of alluvial soils from the easternmost part of the Padanian plain (Northern Italy) within the Po river deltaic system. The new C-N elemental and isotopic data refine previous inferences on the depositional facies, on pedogenetic processes, as well as on anthropogenic influences. Noteworthy, C and N are fundamental elements invariably associated to the SOM and their budget is labile and less stable than that of lithophile elements. Results highlight that the followed approach is useful in the discrimination of the different carbon pools, in particular allowing SOM benchmark of the distinct depositional facies (in subsoils), and to evaluate the effect of agricultural activity on its evolution (in topsoils). Our results indicate that SOM of subsoils is generally affected by microbial degradation that ultimately led to stabilization, with the exception of clayey and peaty deposits that represent carbon reservoir in which biological activity is inhibited and SOM appears relatively preserved. However, the potential greenhouse gas

contribution of the clayey and peaty soils is highlighted by the loss of organic fraction along the soil profiles, which account for ca. 20% of the original budget, plausibly in response to intense agricultural activities. More in general, on the basis of a comparison with historical data, we recorded variable (up to 30%) but ubiquitous losses of the organic fraction throughout the investigated area, over the last eighty years. Global warming can magnify the SOM deterioration (Oertel et al., 2016), and therefore reiteration of similar studies will be useful to monitor the SOM resilience, and to provide indications for sustainable agronomical approaches. In this view, it has to be taken into account that the investigated soils (down to a 100 cm depth) contain an order of 407 tons TOC/ha that if degraded would enhance significantly CO_2 emissions in the atmosphere, an issue that has been investigated at a regional scale by the recent papers of Scalenghe et al. (2011) and Malucelli et al. (2014). Calculations can be extended also to nitrogen species that in the studied soils account for 52 tons TN/ha that could be similarly converted to greenhouse gases. The data recorded by this study therefore represent a snapshot of the current conditions, useful to create a soil geochemical archive as a tool for monitoring natural (climatic) and anthropogenic variations.

Acknowledgements

This study was supported by the European Agricultural Fund for Rural Development (project SaveSOC2, ID: 2017IT06RDEI5015638 v1), allocated by the Emilia-Romagna region (PSR 2014-2020).

References

Agnelli, A., Bol, R., Trumbore, S.E., Dixon, L., Cocco, S., Corti, G., 2014. Carbon and nitrogen in soil and vine roots in harrowed and grass-covered vineyards. Agric. Ecosyst. Environ. 193, 70-82.

Albaladejo, J., Ortiz, R., Garcia-Franco, N., Ruiz Navarro, A., Almagro, M., Garcia Pintado, J., Martinez-Mena, M., 2013. Land use and climate change impacts on soil organic carbon stocks in semi-arid Spain. J. Soil Sediment. 13, 265-277.

Alonso-Zarza, A., Dorado Valiño, M., Valdeolmillos Rodriguez, A., Ruiz Zapata, M.B., 2006. A recent analogue for palustrin carbonate environments: the Quaternary deposits of Las Tablas de Daimiel wetlands, Ciudad Real Spain. Geol. S. Am. S. 416, 153–168.

Amorosi, A., 2012. Chromium and nickel as indicators of source-to-sink sediment transfer in a Holocene alluvial and coastal system (Po Plain, Italy). Sediment. Geol. 280, 260-269.

Amorosi, A., Centineo, M.C., Dinelli, E., Lucchini, F., Tateo, F., 2002. Geochemical and mineralogical variations as indicators of provenance changes in Late Quaternary deposits of SE Po Plain. Sediment. Geol. 151, 273-292.

Bianchini, G., Cremonini, S., Di Giuseppe, D., Vianello, G., Vittori Antisari, L., 2014. Multiproxy investigation of a Holocene sedimentary sequence near Ferrara (Italy): clues on the physiographic evolution of the eastern Padanian Plain. J. Soil Sediment. 14, 230-242.

Bianchini, G., Di Giuseppe, D., Natali, C., Beccaluva, L., 2013. Ophiolite inheritance in the Po plain sediments: insights on heavy metals distribution and risk assessment. Ofioliti 38, 1-14.

Bianchini, G., Natali, C., Di Giuseppe, D., Beccaluva, L., 2012. Heavy metals in soils and sedimentary deposits of the Padanian Plain (Ferrara, Northern Italy): Characterisation and biomonitoring. J. Soil Sediment. 12, 1145-1153.

Bondesan, M., Favero, V., Viñals, M.J., 1995. New evidence on the evolution of the Po Delta coastal plain during the Holocene. Quatern. Int. 29/30, 105–110.

Ciavatta, C., Govi, M., Vittori Antisari, L., Sequi, P., 1990. Characterization of humified compounds by extraction and fractionation on solid polyvynilpyrrolidone. J. Chromatogr. 509, 141-146.

Colombani, N., Salemi, E., Mastrocicco, M., Castaldelli, G., 2011. Groundwater nitrogen speciation in intensively cultivated lowland areas. In: Lambrakis N, Stournaras G, Katsanou K (eds) Advances in the research of aquatic environment. Springer, Berlin, pp 291–298

Dauer, J.M., Perakis, S.S., 2014. Calcium oxalate contribution to calcium cycling in forest of contrasting nutrient status. Forest Ecol. Manag. 334, 64-73.

De Clercq, T., Heiling, M., Dercon, G., Resch, C., Aigner, M., Mayer, L., Mao, Y., Elsen, A., Steier, P., Leifeld, J., Merckx, R., 2015. Predicting soil organic matter stability in agricultural fields through carbon and nitrogen stable isotopes. Soil Biol. Biochem. 88, 29–38.

Di Giuseppe, D., Bianchini, G., Faccini, B., Coltorti, M., 2014a. Combination of wavelength dispersive X-ray fluorescence analysis and multivariate statistic for alluvial soils classification: a case study from the Padanian Plain (Northern Italy). X-Ray Spectrom. 43, 165-174.

Di Giuseppe, D., Bianchini, G., Vittori Antisari, L., Martucci, A., Natali, C., Beccaluva, L., 2014b. Geochemical characterization and biomonitoring of reclaimed soils in the Po River Delta (Northern Italy): implications for the agricultural activities. Environ. Monit. Assess. 186, 2925-2940.

Di Giuseppe, D., Vittori Antisari, L., Ferronato, C., Bianchini, G., 2014c. New insights on mobility and bioavailability of heavy metals in soils of the Padanian alluvial plain (Ferrara Province, northern Italy). Chem. Erde – Geochem. 74, 615-623.

Dunagan, S.P., Turner, C.E., 2004. Regional paleohydrologic and paleoclimatic setting of wetland/lacustrine depositional systems in the Morrison Formation (Upper Jurassic), Western Interior, USA. Sediment. Geol. 167, 269-296.

Dutta, K., Schuur, E.A.G., Neff, J.C., Zimov, S.A., 2006. Potential carbon release from permafrost soils of Northeastern Siberia. Glob. Change Biol. 12, 1-16.

Esmeijer-Liu, A.J., Kürschner, W.M., Lotter, A.F., Verhoeven, J.T.A., Goslar, T., 2012. Stable carbon and nitrogen isotopes in a peat profile are influenced by early stage diagenesis and changes in atmospheric CO_2 and N deposition. Water Air Soil Poll. 223, 2007–2022.

Gonfiantini, R., Stichler, W., Rozanski, K., 1995. Standards and intercomparison materials distributed by the International Atomic Energy Agency for stable isotope measurements, in Reference and Intercomparison Materials for Stable Isotopes of Light Elements, (Stichler W, Ed). IAEA, Vienna, 1993, pp. 13-29.

Hooijer, A., Page, S., Canadell, J.G., Silvius, M., Kwadijik, J., Wosten, H., Jauhiainen, J., 2010 Current and future CO_2 emissions from drained peatland in Southeast Asia. Biogeosciences 7, 1505-1514.

Kovda, I., Morgun, E., Gongalski, K., 2014. Stable isotopic composition of carbonate pedofeatures in soils along a transect in the southern part of European Russia. Catena 112, 56-64.

Kusaka, S., Nakano, T., 2014. Carbon and oxygen isotope ratios and their temperature dependence in carbonate and tooth enamel using GasBench II preparation device. Rapid Commun. Mass Sp. 28, 563–567.

Malucelli, F., Certini, G., Scalenghe, R., 2014. Soil is brown gold in the Emilia-Romagna region, Italy. Land Use Policy 39, 350–357.

Natali, C., Bianchini, G., Vittori Antisari, L., 2018. Thermal separation coupled with elemental and isotopic analysis: A method for soil carbon characterization. Catena 164, 150-157.

Natali, C., Bianchini, G., 2015. Thermally based isotopic speciation of carbon in complex matrices: a tool for environmental investigation. Environ. Sci. Pollut. R. 22, 12162-12173.

Natali, C., Bianchini, G., 2014. Understanding the carbon isotopic signature in complex environmental matrices. Int. J. Environ. Qual. 14, 19–30.

Oertel, C., Matschullat, J., Zurba, K., Zimmermann, F., 2016. Greenhouse gas emissions from soils – A review. Chem. Erde – Geochem. 76, 327-3.

Rumpel, C., Kögel-Knabner, I., 2010. Deep soil organic matter—a key but poorly understood component of terrestrial C cycle. Plant. Soil 338, 143–158.

Scalenghe, R., Malucelli, F., Ungaro, F., Perazzone, L., Filippi, N., Anthony, C., Edwards, C., 2011. Influence of 150 Years of Land Use on Anthropogenic and Natural Carbon Stocks in Emilia-Romagna Region (Italy). Environ. Sci. Technol., 45, 5112–5117.

Simeoni, U., Corbau, C., 2009. A review of the Delta Po evolution (Italy) related to climatic changes and human impacts. Geomorphology 107, 64-71.

Soil Survey Staff -SSS (2010) Keys to Soil Taxonomy. USDA, Natural Resources Conservation Service. Eleventh Edition. 338 p.

Stefani, M., Vincenzi, S., 2005. The interplay of eustasy, climate and human activity in the late Quaternary depositional evolution and sedimentary architecture of the Po Delta system. Mar. Geol. 222–223, 19–48.

Ungaro, F., Ragazzi, F., Cappelin, R., Giandon, P., 2008. Arsenic concentration in the soils of the Brenta plain (Northern Italy): mapping the probability of exceeding contamination thresholds. J. Geochem. Explor. 96, 117–13.

Zamanian, K., Pustovoytov, K., Kuzyakov, Y.. 2016. Pedogenic carbonates: Forms and formation processes. Earth-Sci. Rev. 157, 1–17.

Figure captions:

Fig. 1 – Simplified sedimentological map of the investigated area which is located in the easternmost part of the Padanian plain between the Po and Reno riverine systems. Symbols refer to sample groups identified by cluster analysis and can be roughly ascribed to the related depositional environments. See chapter 4.1 for further details.

Fig. 2 – Total Carbon (TC) and nitrogen (N) versus TC isotope ratio ($\delta^{13}C_{TC}$) of subsoils from the easternmost Padanian plain. Symbols refer to sample groups identified by cluster analysis and can be roughly ascribed to the related depositional environments. Red symbols represent average values for each cluster with the related standard deviation. See chapter 4.1 for further details.

Fig. 3 – Distribution of (a) TC vs CaO, (b) $\delta^{13}C_{TC}$ vs CaO and (c) $\delta^{13}C_{TC}$ vs Sr/Rb of the investigated soils grouped in different clusters; dashed line in (a) represents the calcite stoichiometric line.

Fig. 4 - Carbon elemental and isotopic composition of the different carbon fraction (TC, TIC and TOC) in *A* and *B* soils from the Padanian plain. For the *B* soils the membership to the relative cluster is indicated.

Fig. 6 – C and N isotopic composition of humic and fulvic acids extracted from the investigated *A* and *B* soils. For the *B* soils the membership to the relative cluster is indicated.

Fig. 7 – $\delta^{13}C$ (‰) histograms showing the averaged compositions of bulk SOM (expressed by $\delta^{13}C_{TOC}$) and relative non-extractable (NEOM) and Na-pyrophosphate extractable (EOM = HA+FA) fractions of selected *A* and *B* soils from the easternmost Padanian plain. Bars represent standard deviations.

Supplementary Fig. 1 – Sand-Clay-Silt (%) ternary diagram for textural classification of the investigated soils grouped in different clusters.

Table captions:

Table 1 – Carbon and Nitrogen elemental and isotopic composition and cluster analysis classification of soils from the Padanian deltaic area.

Table 2 – Carbon elemental and isotopic speciation of organic and inorganic carbon pools from selected superficial and deep soils.

Table 3 – Carbon and nitrogen elemental and isotopic composition of organic carbon pools from selected superficial and deep soils.

Supplementary Table 1 – Pedological features of *B* soils from the Padanian deltaic area.

Supplementary Table 2 – Textural analysis of selected *A* and *B* soils from the Padanian deltaic area.

Figure 1

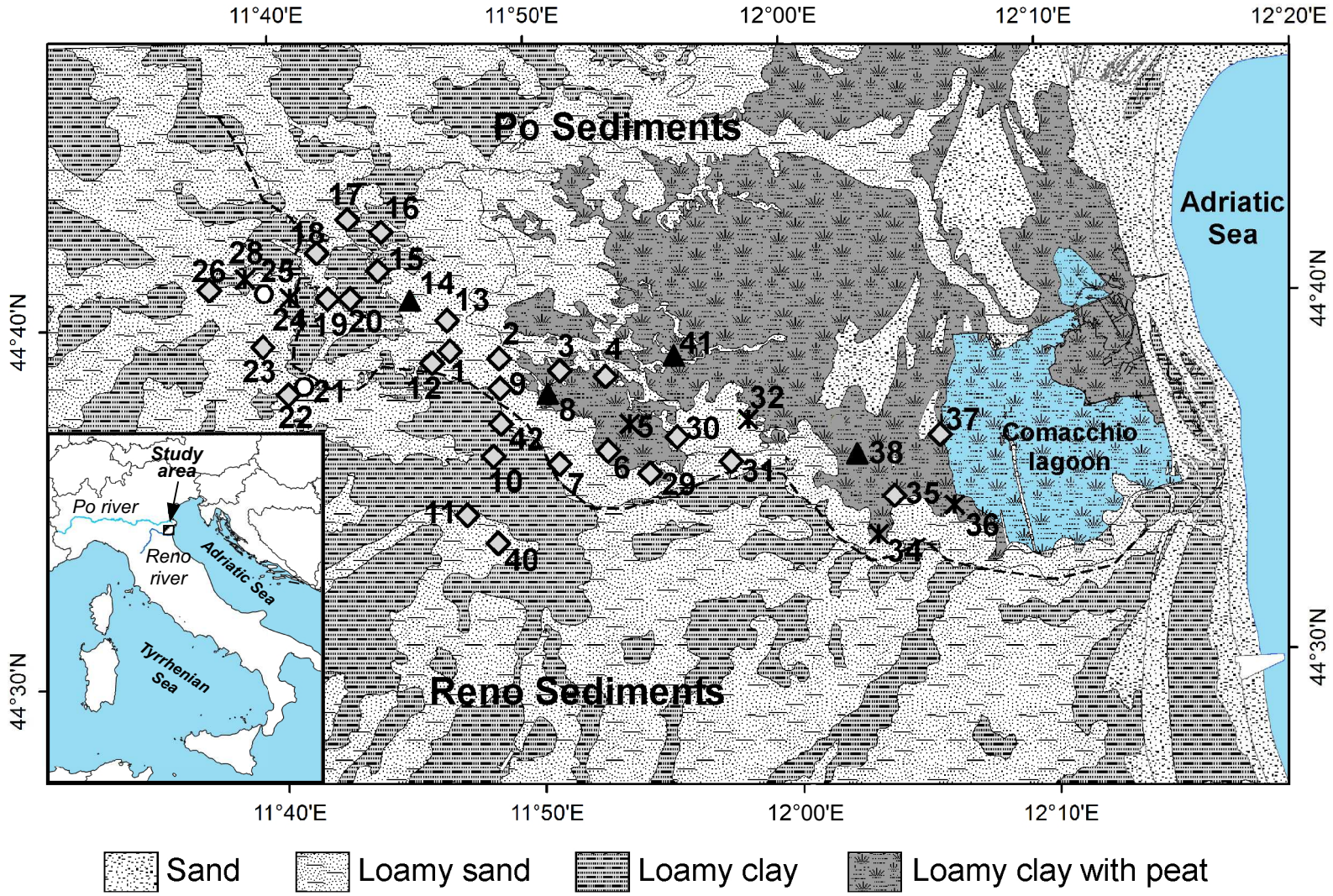
11°40'E
11°50'E
12°00'E
12°10'E
12°20'E
44°40'N
44°30'N
Po Sediments
Reno Sediments
Adriatic Sea
Comacchio lagoon
Study area
Po river
Reno river
Adriatic Sea
Tyrrhenian Sea
Sand
Loamy sand
Loamy clay
Loamy clay with peat

Figure 2

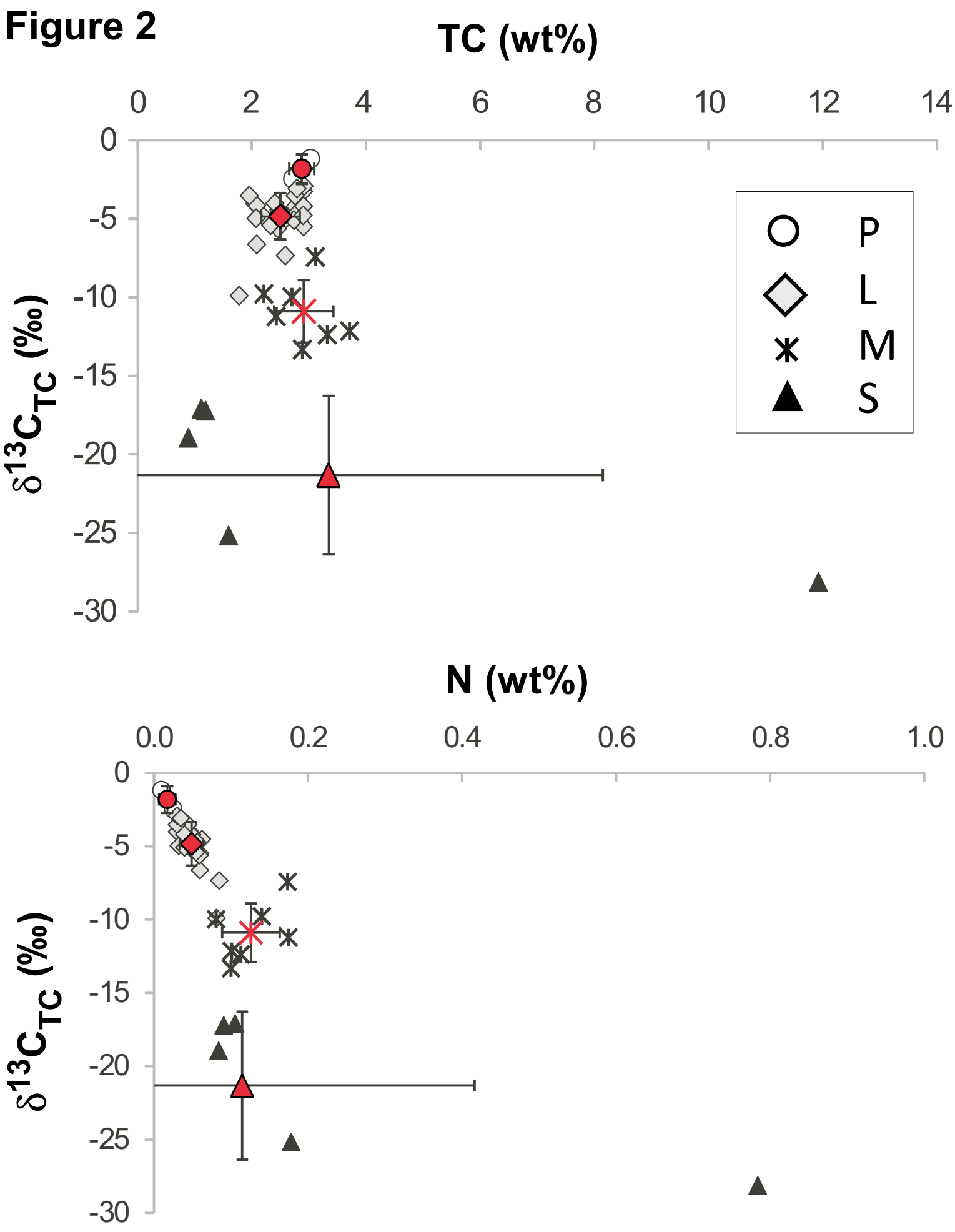
TC (wt%)
0
2
4
6
8
10
12
14
0
-5
-10
-15
-20
-25
-30
δ13CTC (‰)
P
L
M
S
N (wt%)
0.0
0.2
0.4
0.6
0.8
1.0
0
-5
-10
-15
-20
-25
-30
δ13CTC (‰)

Figure 3

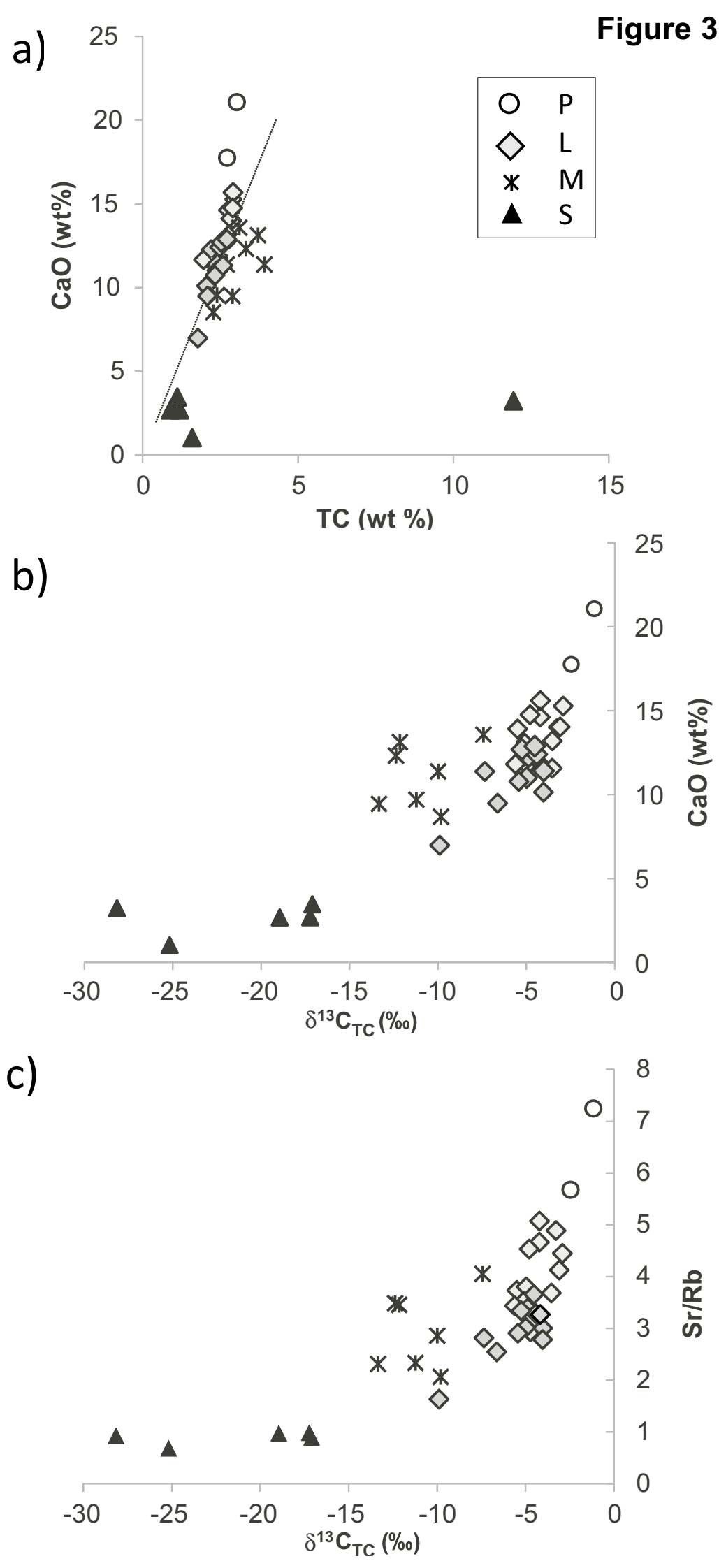

Figure 4

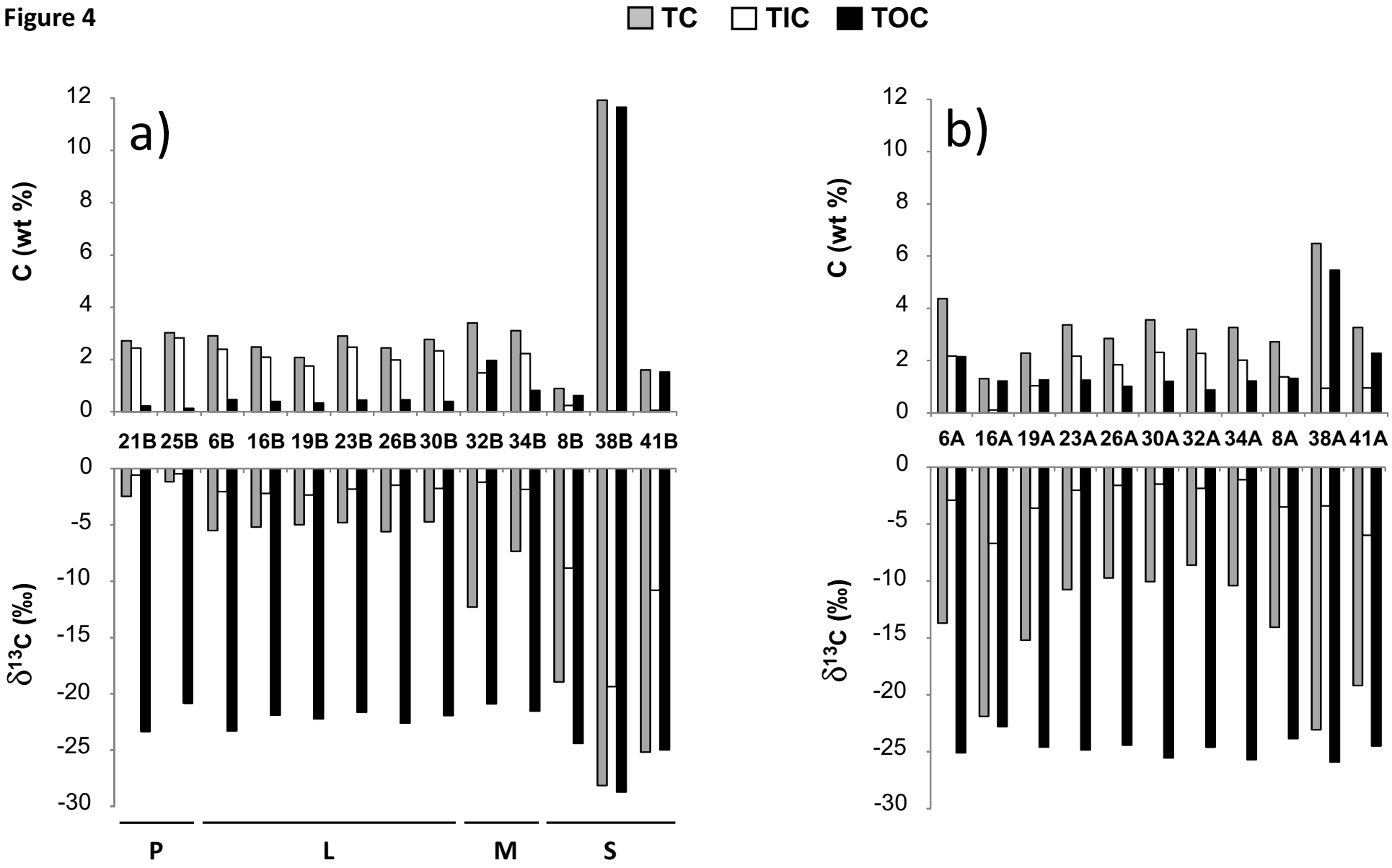
TC
TIC
TOC
a)
b)
C (wt %)
δ13C (‰)
12
10
8
6
4
2
0
-5
-10
-15
-20
-25
-30
21B 25B 6B 16B 19B 23B 26B 30B 32B 34B 8B 38B 41B
6A 16A 19A 23A 26A 30A 32A 34A 8A 38A 41A
P
L
M
S

Figure 5

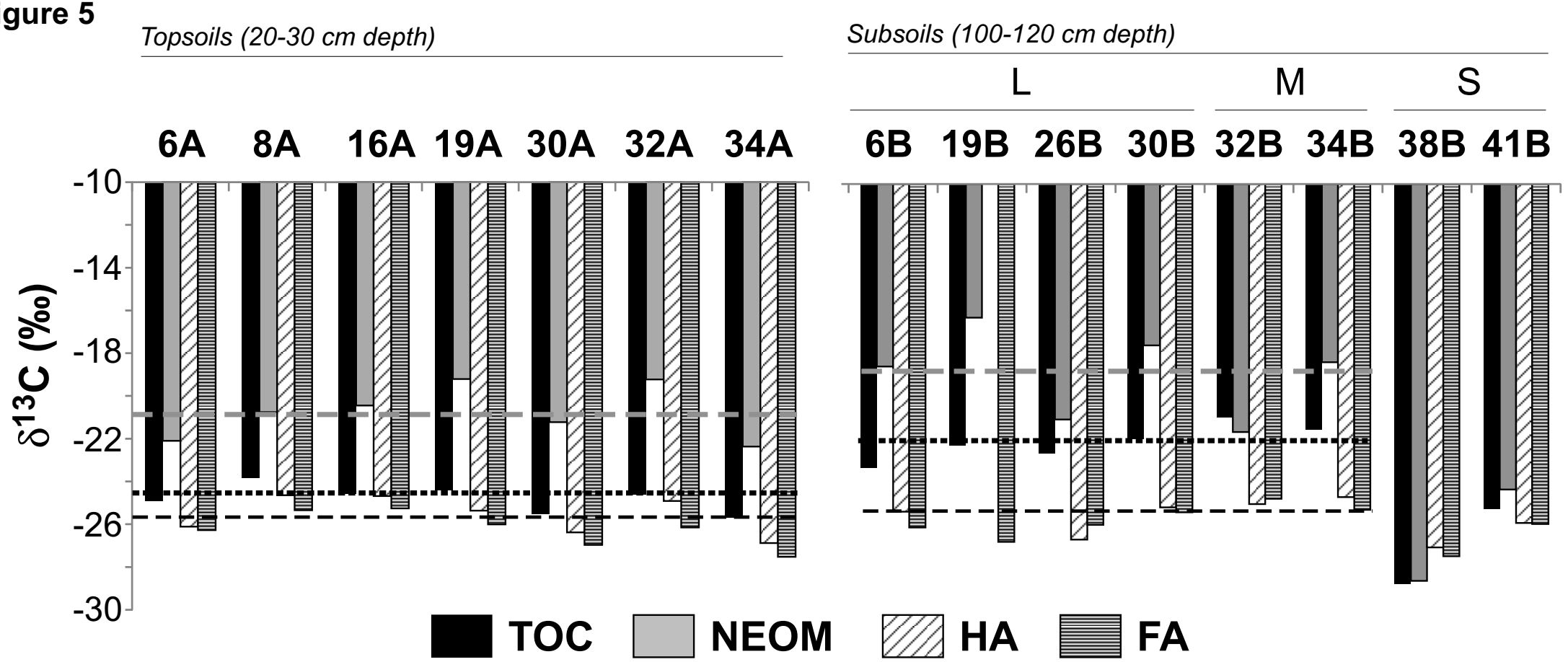
Topsoils (20-30 cm depth)
Subsoils (100-120 cm depth)
L
M
S
6A
8A
16A
19A
30A
32A
34A
6B
19B
26B
30B
32B
34B
38B
41B
-10
-14
-18
-22
-26
-30
δ13C (‰)
TOC
NEOM
HA
FA

Figure 6

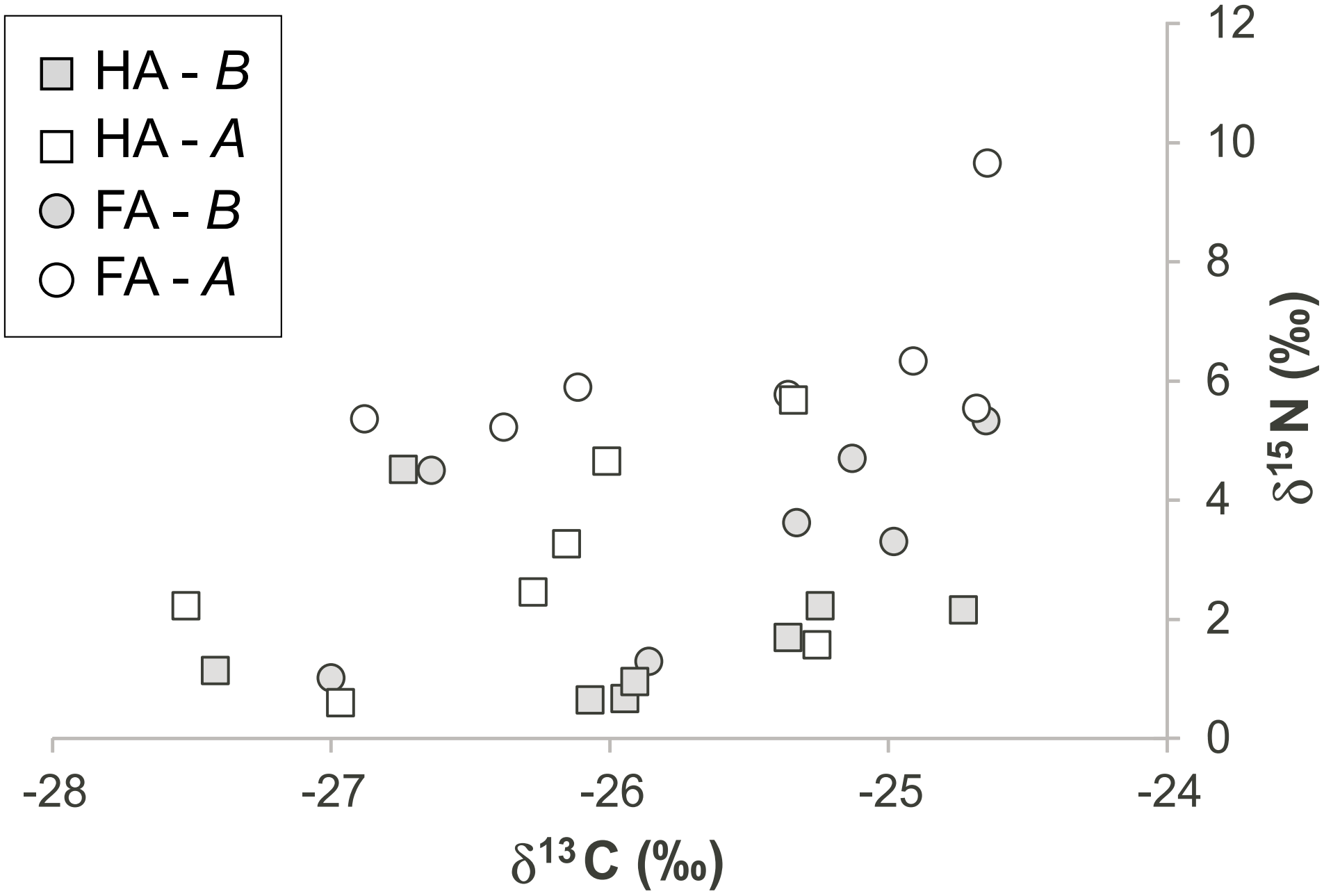

Figure 7

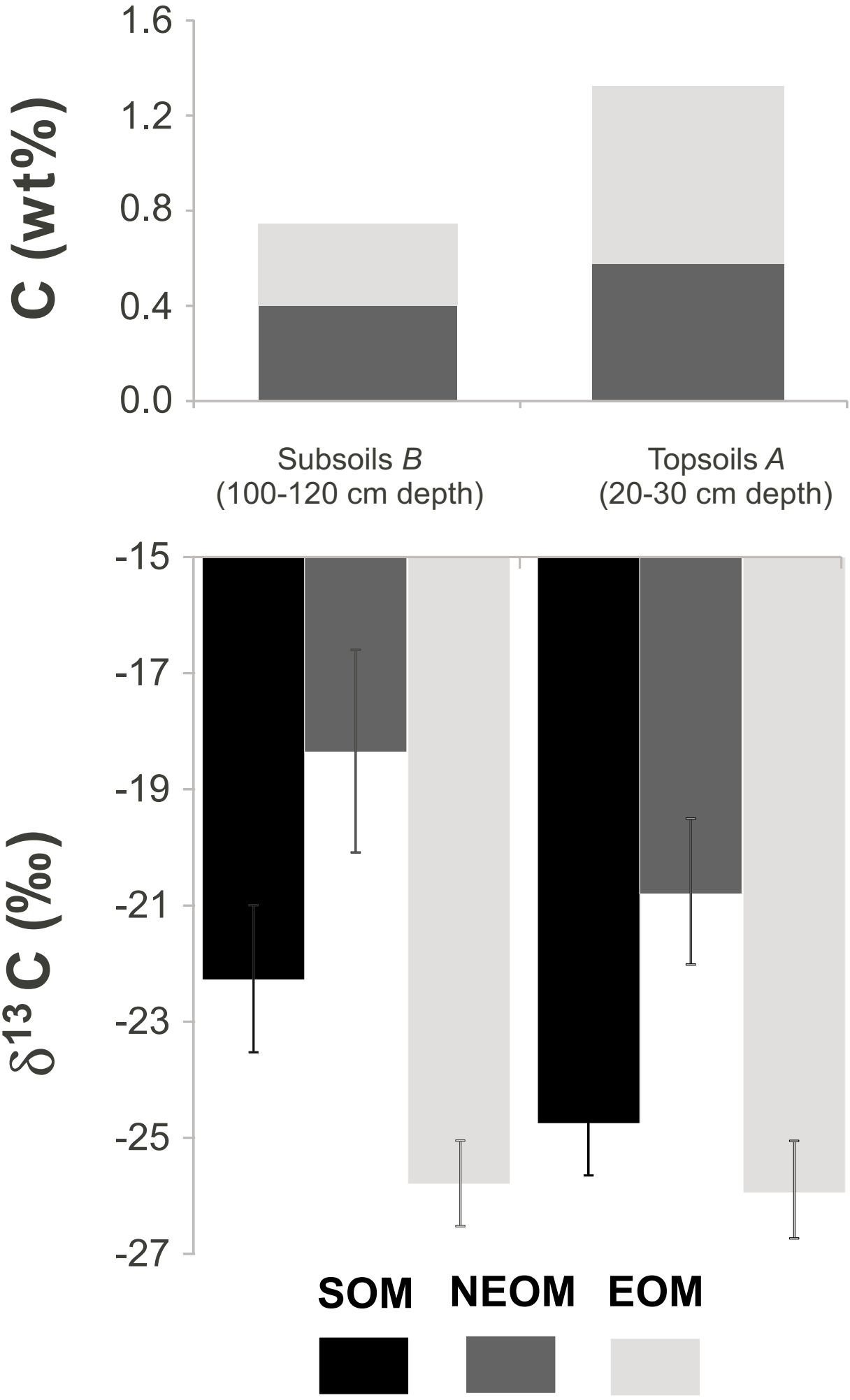
C (wt%)
1.6
1.2
0.8
0.4
0.0
Subsoils *B*
(100-120 cm depth)
Topsoils *A*
(20-30 cm depth)
δ13C (‰)
-15
-17
-19
-21
-23
-25
-27
SOM
NEOM
EOM

Table 1

Sample	TN (wt%)	TC (wt%)	$\delta^{13}C_{TC}$ (‰)	$\delta^{15}N_{TN}$ (‰)	Cluster
100-120 cm depth					
AR1B	0.05	2.39	-5.0	-	L
AR2B	0.05	2.53	-5.3	1.6	L
AR3B	0.04	2.06	-4.0	2.9	L
AR4B	0.06	2.09	-6.6	-	L
AR5B	0.08	2.43	-11.2	-1.2	M
AR6B	0.06	2.91	-5.5	2.8	L
AR7B	0.04	2.91	-3.3	3.7	L
AR8B	0.08	0.89	-19.0	3.8	S
AR9B	0.05	2.09	-4.2	-	L
AR12B	0.06	2.71	-4.5	3.6	L
AR13B	0.08	1.78	-9.9	6.8	L
AR14B	0.11	1.12	-17.1	5.2	S
AR15B	0.05	2.21	-4.9	-0.7	L
AR16B	0.05	2.48	-4.4	1.8	L
AR17B	0.03	2.41	-4.0	-	L
AR18B	0.05	2.76	-4.2	1.6	L
AR19B	0.03	2.08	-5.0	2.9	L
AR20B	0.09	1.19	-17.2	7.1	S
AR29B	0.11	2.70	-10.0	4.7	M
AR30B	0.06	2.77	-4.7	2.4	L
AR31B	0.04	2.74	-5.1	-	L
AR32B	0.17	3.40	-12.3	3.4	M
AR34B	0.10	3.11	-7.4	4.7	M
AR35B	0.05	2.76	-3.5	0.3	L
AR36B	0.14	3.71	-12.2	3.3	M
AR37B	0.03	1.96	-3.5	-	L
AR38B	0.78	11.93	-28.2	1.6	S
AR41B	0.18	1.60	-25.2	3.0	S
AR10B	0.09	2.59	-7.4	2.5	L
AR11B	0.03	2.92	-2.9	1.8	L
AR21B	0.03	2.72	-2.5	3.0	P
AR22B	0.04	2.91	-4.2	-	L
AR23B	0.05	2.90	-4.8	1.8	L
AR24B	0.10	2.21	-9.8	3.8	M
AR25B	0.01	3.03	-1.2	-	P
AR26B	0.06	2.45	-5.6	3.2	L
AR28B	0.18	2.89	-13.3	3.1	M
AR40B	0.04	2.80	-3.1	2.0	L
AR42B	0.06	2.33	-5.4	2.4	L
20-30 cm depth					
AR6A	0.22	4.37	-13.7	4.1	
AR8A	0.19	2.84	-14.1	8.2	
AR16A	0.16	1.31	-21.9	4.9	
AR23A	0.16	3.37	-10.8	5.2	
AR26A	0.15	2.85	-9.7	5.0	
AR19A	0.16	2.29	-15.2	7.6	
AR30A	0.14	3.56	-10.1	4.9	
AR32A	0.11	3.20	-8.6	4.3	
AR34A	0.15	3.27	-10.4	4.5	
AR38A	0.45	6.49	-23.1	3.4	
AR41A	0.28	3.27	-19.2	10.0	

Table 2

		Measured									
		TC		TIC		TOC		Recovery (TC-TIC+TOC)			
Sample	**LOI**	**C (wt%)**	**$\delta^{13}C$ (‰)**	**C (wt%)**	**$\delta^{13}C$ (‰)**	**C (wt%)**	**$\delta^{13}C$ (‰)**	**C (%)**	**$\Delta^{13}C$ (‰)**	**$\Delta^{13}C_{TIC-TOC}$ (‰)**	**Cluster**
100-120 cm depth											
21B	2.31	2.72	-2.5	2.44	-0.6	0.22	-23.4	98	0.0	*-22.8*	P
25B	1.36	3.03	-1.2	2.83	-0.5	0.13	-20.9	98	0.2	*-20.4*	P
6B	6.54	2.91	-5.5	2.39	-2.0	0.47	-23.3	98	0.0	*-21.3*	L
16B	5.30	2.48	-5.2	2.09	-2.2	0.4	-21.9	101	0.2	*-19.7*	L
19B	3.52	2.08	-5.0	1.76	-2.3	0.34	-22.2	101	0.6	*-19.9*	L
23B	4.39	2.90	-4.8	2.48	-1.8	0.45	-21.6	101	0.1	*-19.8*	L
26B	4.61	2.45	-5.6	1.98	-1.5	0.46	-22.6	100	-0.1	*-21.1*	L
30B	5.08	2.77	-4.7	2.33	-1.8	0.40	-21.9	99	0.0	*-20.2*	L
32B	9.71	3.40	-12.3	1.49	-1.2	1.97	-20.9	102	0.1	*-18.6*	M
34B	7.59	3.11	-7.4	2.23	-1.9	0.82	-21.5	98	-0.2	*-17.2*	M
8B	9.19	0.89	-19.0	0.28	-8.8	0.61	-24.4	100	0.6	*-15.6*	S
38B	30.10	11.9	-28.2	0.03	-19.4	11.7	-28.7	98	0.5	*-9.3*	S
41B	9.95	1.60	-25.2	0.06	-10.8	1.52	-25.0	99	-0.7	*-11.3*	S
20-30 cm depth											
6A	9.29	4.37	-13.7	2.18	-2.9	2.15	-25.1	99	0.2	*-21.7*	
16A	10.74	1.31	-21.9	0.11	-6.7	1.22	-22.8	102	-0.4	*-12.9*	
19A	6.82	2.29	-15.2	1.04	-3.6	1.26	-24.6	100	-0.1	*-20.6*	
23A	6.11	3.37	-10.8	2.17	-2.0	1.25	-24.8	101	-0.4	*-22.8*	
26A	6.69	2.85	-9.7	1.84	-1.6	1.02	-24.4	100	0.0	*-22.8*	
30A	5.48	3.56	-10.1	2.32	-1.5	1.21	-25.5	99	-0.3	*-24.1*	
32A	5.01	3.20	-8.6	2.28	-1.9	0.88	-24.6	99	-0.4	*-22.8*	
34A	4.25	3.27	-10.4	2.02	-1.1	1.22	-25.7	99	0.0	*-24.4*	
8A	7.76	2.72	-14.1	1.38	-3.5	1.32	-23.8	99	-0.6	*-20.3*	
38A	5.67	6.49	-23.1	0.94	-3.4	5.47	-25.9	99	-0.5	*-24.4*	
41A	14.8	3.27	-19.2	0.95	-6.0	2.28	-24.5	99	-0.1	*-23.4*	

Table 3

	Soil Organic Matter (SOM)										
	NEOM		HA				FA				
Sample	**C (wt%)**	**δ^{13}C (‰)**	**C (wt%)**	**δ^{13}C (‰)**	**N (wt%)**	**δ^{15}N (‰)**	**C (wt%)**	**δ^{13}C (‰)**	**N (wt%)**	**δ^{15}N (‰)**	**Cluster**
100-120 cm depth											
6B	0.36	-18.5	36.4	-25.3	3.02	3.6	46.8	-26.1	4.11	0.6	L
19B	0.15	-16.3	-	-	-	-	38.2	-26.7	3.41	4.5	L
26B	0.46	-21.0	41.8	-26.6	3.29	4.5	37.4	-25.9	2.84	0.7	L
30B	0.32	-17.6	41.3	-25.1	3.13	4.7	28.0	-25.4	1.60	1.7	L
32B	0.66	-21.6	42.8	-25.0	3.34	3.3	35.9	-24.7	2.41	2.2	M
34B	0.45	-18.3	33.6	-24.7	3.11	5.3	39.8	-25.2	3.03	2.2	M
38B	4.83	-28.6	37.1	-27.0	2.62	1.0	36.7	-27.4	1.59	1.1	S
41B	1.08	-24.3	42.1	-25.9	3.36	1.3	38.0	-25.9	2.83	1.0	S
20-30 cm depth											
6A	0.88	-22.1	37.6	-26.1	3.15	5.9	33.8	-26.3	2.25	2.5	
8A	0.67	-20.8	30.3	-24.6	2.91	9.7	38.2	-25.3	3.15	5.7	
16A	0.47	-20.5	27.5	-24.7	2.37	5.5	36.0	-25.3	3.20	1.6	
19A	0.41	-19.2	40.7	-25.4	3.74	5.8	38.8	-26.0	2.96	4.7	
30A	0.55	-21.2	42.5	-26.4	3.42	5.2	36.9	-27.0	2.77	0.6	
32A	0.42	-19.2	42.2	-24.9	3.98	6.3	36.6	-26.2	2.62	3.3	
34A	0.65	-22.4	42.1	-26.9	4.11	5.4	39.8	-27.5	3.03	2.2	

Supplementary Figure 1

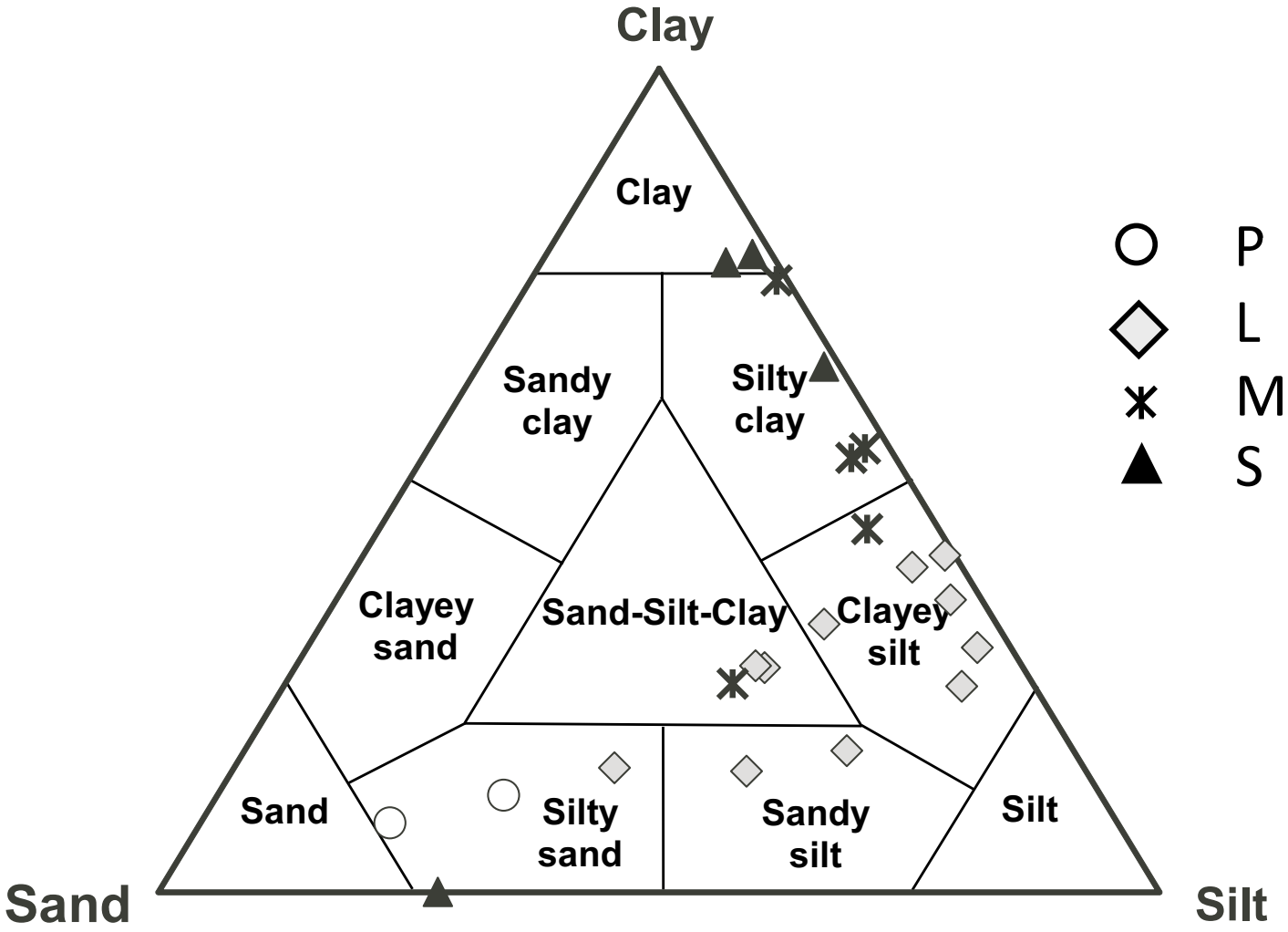

Supplementary Table 1

Sample	Soil Taxonomy	Soil Horizon
100-120 cm depth		
AR1B	(2010) Aquic Haplustepts coarse silty, mixed, superactive, mesic	BW2-C
AR2B	(2010) Aquic Haplustepts coarse silty, mixed, superactive, mesic	BW2-C
AR3B	(2010) Aquic Haplustepts coarse silty, mixed, superactive, mesic	Bw(g)/C-Oa/(2)Cg
AR4B	(2010) Sulfic Endoaquepts fine, mixed, superactive, calcareous, mesic	Cg/Oe
AR5B	(2010) Sulfic Endoaquepts fine, mixed, superactive, calcareous, mesic	Cg/Oe
AR6B	(2010) Sulfic Endoaquepts fine, mixed, superactive, calcareous, mesic	Cg/Oe
AR7B	(2010) Aquic Haplustepts coarse silty, mixed, superactive, mesic	BW2-C
AR8B	(2010) Aquic Haplustepts coarse silty, mixed, superactive, mesic	Bw(g)/C-Oa/(2)Cg
AR9B	(2010) Aquic Haplustepts coarse silty, mixed, superactive, mesic	BW2-C
AR12B	(2010) Aquic Haplustepts fine silty, mixed, superactive, mesic	BC(g)-Bg(ss)
AR13B	(2010) Aquic Haplustepts coarse silty, mixed, superactive, mesic	BW2-C
AR14B	(2010) Aquic Calciusteps fine silty, mixed, superactive, mesic	Bk
AR15B	(2010) Udifluventic Haplustepts, fine, mixed, active, mesic	Bk(g)/BCk(g)-2Bkg/2BCyg
AR16B	(2010) Udifluventic Haplustepts, fine, mixed, active, mesic	Bk(g)/BCk(g)-2Bkg/2BCyg
AR17B	(2010) Aquic Calciusteps fine silty, mixed, superactive, mesic	Bk
AR18B	(2010) Aquic Haplustepts coarse silty, mixed, superactive, mesic	BW2-Bk/BC
AR19B	(2010) Aquic Haplustepts coarse silty, mixed, superactive, mesic	BW2-Bk/BC
AR20B	(2010) Udifluventic Haplustepts, fine, mixed, active, mesic	Bk(g)/BCk(g)-2Bkg/2BCyg
AR29B	(2010) Aquic Haplustepts coarse silty, mixed, superactive, mesic	BW2-C
AR30B	(2010) Aquic Haplustepts coarse silty, mixed, superactive, mesic	Bw(g)/C-Oa/(2)Cg
AR31B	(2010) Aquic Haplustepts coarse silty, mixed, superactive, mesic	BW2-C
AR32B		Cg2
AR34B	(2010) Aquic Haplustepts coarse silty, mixed, superactive, mesic	BW2-C
AR35B	(2010) Sulfic Endoaquepts fine, mixed, superactive, calcareous, mesic	Cg/Oe
AR36B	(2010) Sulfic Endoaquepts fine, mixed, superactive, calcareous, mesic	Cg/Oe
AR37B	(2010) Taphto-Histic Endoaquolls loamy, mixed, superactive, calcareous, mesic	2Cg
AR38B	(2010) Aquic Ustipsamments, mixed, mesic	C2/Cg-Cg
AR41B	(2010) Sulfic Endoaquepts fine, mixed, superactive, calcareous, mesic	Cg/Oe-Cg
AR10B	(2010) Vertic Endoaquepts fine, mixed, active, calcareous, mesic	Cg(ss)
AR11B	(2010) Udifluventic Haplustept fine silty, mixed, superactive, mesic	C-BC(g)
AR21B	(2010) Oxyaquic Ustifluvents fine silty, mixed, active, calcareous, mesic	C-C2
AR22B	(2010) Oxyaquic Ustifluvents fine silty, mixed, active, calcareous, mesic	C-C2
AR23B	(2010) Udifluventic Haplustept coarse loamy, mixed, superactive, mesic	C
AR24B	(2010) Ustic Endoaquerts fine, mixed, active, mesic	Bss(g)/AC-CG(ss)
AR25B	(2010) Udifluventic Haplustept fine silty, mixed, superactive, mesic	C-C
AR26B	(2010) Udifluventic Haplustept coarse loamy, mixed, superactive, mesic	C-C2
AR28B	(2010) Aquic Haplustepts fine silty, mixed, superactive, mesic	BC(g)
AR40B	(2010) Udifluventic Haplustept fine silty, mixed, superactive, mesic	C-C2
AR42B	(2010) Vertic Endoaquepts fine, mixed, active, calcareous, mesic	Cg(ss)

Supplementary Table 2

Sample	Sand	Silt	Clay
100-120 cm depth			
AR6B	1	58	41
AR8B	2	35	64
AR16B	4	67	29
AR18B	7	68	25
AR19B	22	59	17
AR20B	2	21	77
AR30B	5	56	39
AR32B	30	45	25
AR34B	7	49	44
AR35B	47	38	15
AR36B	4	43	53
AR37B	34	51	15
AR38B	72	28	0
AR41B	5	18	76
AR21B	60	29	12
AR22B	27	46	27
AR23B	17	50	32
AR24B	1	25	75
AR25B	73	19	8
AR26B	26	47	27
AR28B	1	46	53
AR40B	3	61	35
20-30 cm depth			
AR6A	10	52	38
AR8A	12	49	39
AR16A	32	33	35
AR23A	29	42	28
AR26A	12	50	38
AR19A	25	49	25

References:

Shepard, F.P., 1954, Nomenclature based on sand-silt-clay ratios: Journal of Sedimentary Petrology, v. 24, p. 151-158

Wentworth, C.K. (1922) A scale of grade and class terms for clastic sediments. Journal of Geology, 30, 377-392.